

# Climate Change Impacts on Surface Runoff in the Hyrcanian Forests

H. R. Moradi, K. C. Abbaspour

**Abstract**— The Hyrcanian forests are green belt stretching over the northern slopes of the Alborz mountain ranges and cover the southern coasts of the Caspian Sea. The climate of this region is controlled by several components of a regional atmospheric circulation pattern and is strongly modulated by a complex topography and the maritime effect of the Caspian Sea. Climate change will accelerate the hydrologic cycle, altering rainfall, and the magnitude and timing of runoff. Hyrcanian forests might become one of the most vulnerable areas in the world regarding climate change. Therefore, the purpose of this paper is to assess the impacts of climate change on surface runoff from the Hyrcanian forests in the North of Iran. To study the effects of climatic variations, the SWAT model was implemented to simulate the hydrological regime and the SUFI-2 algorithm was used for parameter optimization. The climate change scenarios were constructed using outcomes of three General Circulation Models (CGCM2, HadCM3, and SCIRO2) for three emission scenarios (A1F1, A2 and B1) by adjusting the baseline climatic variables that represent the current precipitation and temperature patterns. The study results for 2040-2069 compared with the present climate showed changes in surface runoff by -1.3%, 5% and -1.2% for the A1F1, A2 and B1 scenarios, respectively. Monthly variations show pronounced increases in discharge in the wet season (February-May) and decrease in dry season (July-September). The results highlight the strong impact of climate change in surface runoff and reflect the importance of incorporating such analysis into adaptive management.

**Index Terms**— Climate Change, Hyrcanian Forests, Surface Runoff, SWAT, SWAT –CUP, Iran.

## I. INTRODUCTION

Hyrcanian forests stretch out from sea-level up to an altitude of 2,800 m and encompass different forest types by the virtue of their 80 different woody species (trees and shrubs). The area is rich in hardwood species, but there are only four genera of endemic softwood (conifer) trees including yew, Greek juniper, oriental arbor-vitae and Italian cypress. However, based on the studies of Fadaiey Khojasteh et al. (2010) three genera of Mesozoic Gymnosperms were recognized. The primary function of the Hyrcanian forests, other than wood production, is supportive and environmental. They play a vital role in the conservation of soil and water resources and keep nature at balance on these susceptible steep mountain slopes. However, rapid urbanization and industrialization, intensive grazing, over-utilization of forests for firewood production and farming is destabilizing the forest and the environments around it.

**H. R. Moradi**, Associate Professor Department of Watershed Management Engineering, College of Natural Resources, Tarbiat Modares University (TMU), Noor, Mazandaran Province, Iran, phone number, 00981144553101, Fax, 00981144553499, P.O. Box 46417-76489,

**K. C. Abbaspour**, Eawag, Swiss Federal Institute of Aquatic Science and Technology, P.O. Box 611, 8600 Dübendorf, Switzerland

Over the last few decades, swift forest degradation has brought about a number of environmental, social and economic impacts including soil erosion, floods, degradation of farmlands and habitats, reduction of biodiversity and natural resources, and air and water pollution. Furthermore, manipulation of forest ecosystems has threatened a number of animal species such as fallow deer, roe deer, wolf, fox, wild cat, leopard, pheasant and trout.

In recent years, climate change is one of the most important phenomena that threatens this unique ecosystem. The consensus of atmospheric scientists is that the earth is warming, and as global temperatures increase, the hydrologic cycle is becoming more vigorous. The IPCC has reported that there has been a very likely increase (probability 90–99%) in precipitation during the 20th century in the mid-to-high latitudes of the Northern Hemisphere. According to the Fourth Assessment Report (AR4) of IPCC, global mean surface temperature, precipitation and extreme events such as heavy precipitation and droughts have changed significantly, and the changes are very likely to continue (IPCC 2007). The rises of earth near-surface air temperature and changes in precipitation patterns are prominent features of climate change; these two factors impact almost all other hydrological processes. All Atmospheric-Ocean General Circulation Models (AOGCMs) predict a rise in earth surface temperature and rainfall intensity and amount due to increasing in greenhouse gasses (GHG) concentration over the coming century (Kaini et al. 2010).

A warmer climate will accelerate the hydrologic cycle, altering rainfall, magnitude, and timing of runoff. Warm air holds more moisture and increases evaporation of surface moisture. With more moisture in the atmosphere, rainfall and snowfall events tend to be more intense, increasing the potential for floods (Dhar and Mazumdar 2009). Using present day precipitation patterns, studies have shown that higher temperatures lead to increased evaporation rates, reductions in surface runoff, and increased the frequency of droughts (Ficklin et al. 2009). The changes in flow characteristics resulting from climate change depend on individual catchment characteristics. In particular, basin geology and elevation are first-order controls on the timing and magnitude of basin runoff to climate change (Hamlet and Lettenmaier 2007). Nearly all regions of the world are expected to experience a net negative impact of climate change on water resources. But the intensity and characteristics of the impact, however, can vary significantly from region to region (Abbaspour et al. 2009). Reliable predictions of the quantity and rate of runoff are needed to help decision makers in developing watershed management plans for better soil and water conservation measures.

Many recent studies have focused on the potential effects of climate change on water resources including water quality and

quantity. Gosain et al (2006) simulated the impacts of a 2041–2060 climate change scenario on stream discharges from 12 major river basins in India, ranging in size from 1,668 to 87,180 km<sup>2</sup>. Stream discharge was found to generally decrease, and the severity of both floods and droughts increased in response to the climate change projection. Aimed to the prediction of surface runoff in the upper Mississippi River basin, Jha et al (2006) used various global climate models to predict surface runoff in the upper Mississippi River basin. Study results showed a wide range of changes, from a 6% decrease to a 51% increase depending primarily on precipitation patterns. Abbaspour et al (2009) used the hydrologic program Soil and Water Assessment Tool (SWAT) (Arnold et al. 1998) to study the impact of future climate on water resources availability in Iran. Future climate scenarios for periods of 2010–2040 and 2070–2100 were generated from the Canadian Global Coupled Model (CGCM 3.1) for scenarios A1B, B1, and A2. Analysis of daily rainfall intensities indicated more frequent and larger-intensity floods in the wet regions and more prolonged droughts in the dry regions. Chang and Jung (2010) estimated potential changes in annual, seasonal, and high and low runoff and associated uncertainty in the 218 sub-basins of the Willamette River basin of Oregon. The seasonal variability of runoff is projected to increase consistently with increases in winter flow and decreases in summer flow. Zarghami et al (2011) used LARS-WG and General Circulation Models (GCM) outputs for prediction the climate change on the East Azerbaijan Province in Iran. The research outcomes using the artificial neural network (ANN), showed dramatic reductions in the flows. Azari et al (2015) simulated the impacts of a 2040–2069 climate change impacts on surface runoff in Gorganroud river basin in the North of Iran. The study results showed an increase in annual surface runoff of 5.8%, 2.8% and 9.5% and an increase in sediment yield of 47.7%, 44.5% and 35.9% for the A1F1, A2, and B1 emission scenarios, respectively.

The above studies indicate that watershed processes are very sensitive to changes in precipitation and temperature and can vary significantly from region to region. Therefore, quantifying Hydrological impacts of Climate Change and future conditions will be valuable in understanding and predicting discharge processes as well as watershed-scale sustainable water management. The potential future changes in sediment load Also should be seen as an important requirement for sound river basin management. In this study, we evaluate the potential impacts of climate changes on surface runoff in the Hyrcanian forests in the north of Iran. For this purpose, we used SWAT to simulate the surface runoff with three AOGCS climate models (CGCM2, CSIRO, and HadCM3) for the time period of 2040–2069 under A1F1, A2 and B1 greenhouse gas emissions scenarios. This paper contributes to the scientific understanding of changing surface runoff in this region.

## II. MATERIAL AND METHODS

### 2.1 Study Area

The Hyrcanian forest stretches from Astara in the northwest to the Gorgan vicinity in the northeast of Iran. This area is approximately 800 km long and 110 km wide and has a total

area of 18,500 km<sup>2</sup> comprising 15 % of the total Iranian forests and 1.1 % of the country's area.

The study region located between 35° 47'–36° 35' N and 50° 34'–54° 10' E in the Mazandaran province (Figure 1). Agriculture, forests, and range lands dominants the land use. The elevation ranges from -26m at the outlet to 5595 m at the top of Damavand peak in the south of the area. The annual rainfall varies from 231 mm to 1200 mm. The minimum and the maximum temperatures in the province ranges from 9°C and 18.1°C, respectively. The temperature of the warmest month ranges from 28 to 35 °C while that of the coldest month is between 1.5 and 4 °C. Summer temperature ranges between 20 and 30 °C.

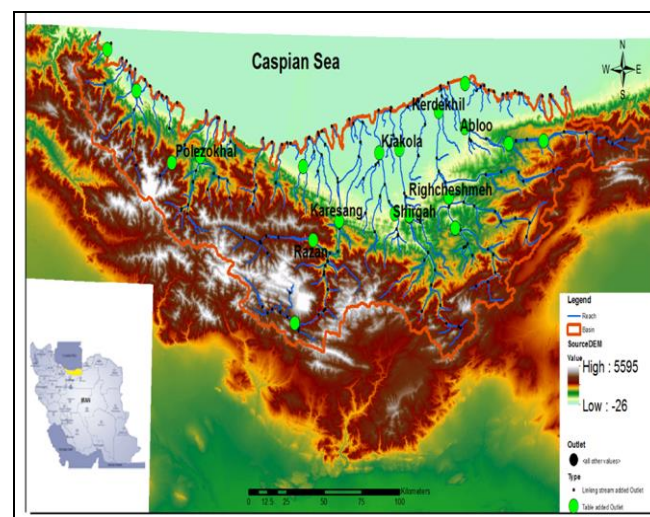


**Fig. 1** Location of the part of Hyrcanian forests in the Mazandaran province

### 2.2 The SWAT Model

The Soil and Water Assessment Tool (SWAT) (Arnold et al. 1998) is a physical process based model to simulate continuous-time landscape processes at a catchment scale. In SWAT watershed is divided into hydrological response units (HRUs) based on soil type, land use and slope classes that allow a high level of spatial detail simulation. The major model components include hydrology, weather, soil erosion, nutrients, soil temperature, crop growth, pesticides agricultural management and stream routing. The model predicts the hydrology at each HRU using the water balance equation, which includes daily precipitation, runoff, evapotranspiration, percolation and return flow components. The surface runoff is estimated in the model using two options (i) the Natural Resources Conservation Service Curve Number (CN) method and (ii) the Green and Ampt method. The percolation through each soil layer is predicted using storage routing techniques combined with the crack-flow model. The evapotranspiration is estimated in SWAT using three options (i) Priestley-Taylor, (ii) Penman-Monteith and (iii) Hargreaves. The flow routing in the river channels is computed using the variable storage coefficient method, or Muskingum method (Arnold et al. 1998). The wide range of SWAT applications underscores that the model is a very flexible and robust tool that can be used to simulate a variety of watershed problems. Hence SWAT was selected for use in this study because of its ability to simulate regional water flow at a watershed scale and to provide effective results.

## 2.3 Data and Model setup

Land use map extracted from the interpretation of Land sat TM (30m resolution) satellite imagery, based on field investigation, which contains seven different land use classes. Soil map and texture was obtained from Iranian ministry of Agriculture which has a spatial resolution of 1:250,000 and includes a set of estimated physical and chemical soil properties. The catchment area of the Mazandaran province was delineated and discretized into sub-basins using a 30m DEM. Daily observed climate data including daily precipitation and temperature were obtained for 25 stations from the Iranian Meteorological Organization and the Water Resources Management Organization (WRMO) of Iran. Daily river discharge data required for calibration-validation were obtained from the WRMO of Iran. The monthly discharge data from 20 hydrometric stations within the basin for 34 years were used for model calibration and validation. Three slope classes including 0-15, 15-30, 30-60 were used in HRU definition. With these specifications, a total of 372 sub basins and 2535 HRUs were delineated in the study area.

## 2.4 Calibration and sensitivity analysis

Parameter optimization and uncertainty analysis were done using the Sequential Uncertainty Fitting Program SUFI-2 (Abbaspour, 2007). In this algorithm, all uncertainties (parameter, conceptual model, input, etc.) are mapped onto the parameter ranges as the procedure tries to capture most of the measured data within the 95% prediction uncertainty (95PPU). Two indices were used to quantify the goodness of calibration/uncertainty performance. Two indexes define the strength of calibration and the prediction uncertainty: P-factor, which is the percentage of data bracketed by the 95PPU band (maximum value 100%), and the R-factor, which is the average width of the band 95PPU divided by the standard deviation of the corresponding measured variable. Model evaluation is an essential measure to verify the robustness of the model. The performance of the model for simulating discharge is evaluated by Nash-Sutcliffe efficiency ( $E_{NS}$ ) (Eq. 1), and the coefficient of determination ( $R^2$ ) (Eq. 2).  $E_{NS}$  ranges from negative infinity to 1, with 1 denoting a perfect model agreement with observation (Nash and Sutcliffe 1970).

$$E_{NS} = \frac{\sum_{i=1}^n (Y_{i, sim} - Y_{i, obs})^2}{\sum_{i=1}^n (Y_{i, obs} - \bar{Y}_{obs})^2} \quad (1)$$

$$R^2 = \frac{\left( \sum_{i=1}^n (Y_{i, obs} - \bar{Y}_{obs})(Y_{i, sim} - \bar{Y}_{sim}) \right)^2}{\sum_{i=1}^n (Y_{i, obs} - \bar{Y}_{obs})^2 \sum_{i=1}^n (Y_{i, sim} - \bar{Y}_{sim})^2} \quad (2)$$

In these equations,  $n$  is number of observed data,  $Y_{i, obs}$  and  $Y_{i, sim}$  are observed and simulated data, respectively, on each time step  $i$  (e.g., day or month),  $\bar{Y}_{obs}$  and  $\bar{Y}_{sim}$  are mean values for observed and simulated data, respectively. We considered 1972–1996 and 1997–2006 as the simulation periods for calibration and validation, respectively. The first two years was considered as a warm-up period in which the model was allowed to initialize and approach reasonable initial values for model state variables.

## 2.5 Future Climate Data

A common approach for assessing future runoff conditions is to use climate model projections in combination with hydrological models. In this study, we used data from climate simulations statistically downscaled by the Climatic Research Unit, University of East Anglia. The three Global Climate Models (GCM) used were: CGCM2 (Coupled Global Climate Model) from Canadian Center for Climate Modeling and Analysis, HadCM3 from Hadley Centre for Climate Prediction and Research and SCIRO2 from Australia's Commonwealth Scientific and Industrial Research Organization. Scenarios with the highest (A1FI scenario – 970 ppm by 2100), lowest (B1 scenario – 550 ppm by 2100) and plausible (A2 scenario – 845 ppm by 2100) projected CO<sub>2</sub> concentrations were chosen for this study. Monthly maximum temperature, minimum temperature, and precipitation on a 0.5° grid are available for globe from 2001 to 2100 (Mitchell et al. 2004).

Climate change scenarios were developed using downscaled monthly average total precipitation and monthly mean temperature data. The baseline data was from 1971–2000. Initially, the GCM gridded data were spatially interpolated to the target stations using inverse distance weighted averaging of four native neighbors. Taking the center as the grid point for each grid box, we used.

$$S_i = \sum_{k=1}^4 \left[ \frac{1}{d_{i,k}^m} \left( \sum_{j=1}^4 \frac{1}{d_{i,j}^m} \right)^{-1} p_k \right] \quad (3)$$

Where  $S_i$  is the downscaled site-specific GCM projection at site  $i$ ,  $p_k$  is the GCM projection at the cell  $k$ ,  $d_{i,k}$  is the distance between site  $i$  and the center of cell  $k$ ,  $m=3$  is used in this study (Liu and Zuo, 2012). Then Change Factor (CF) method was used to generate climate change scenarios for 2040–2069. The CF method involves adjusting the observed daily temperature ( $T_{obs,d}$ ) by adding the difference in monthly temperature predicted by the climate model (GCM or RCM) between the future and the reference period ( $T_{CM,fut,m} - T_{CM,ref,m}$ ). To obtain daily temperature at the future horizon ( $T_{adj,fut,d}$ ) we used Eq. 4. The adjusted daily precipitation for the future horizon ( $P_{adj,fut,d}$ ) is obtained by multiplying the precipitation ratio ( $P_{CM,fut,m}/P_{CM,ref,m}$ ) with the observed daily precipitation ( $P_{obs,d}$ ) (Eq. 5) (Chen et al. 2011).

$$T_{adj,fut,d} = T_{obs,d} + (\bar{T}_{CM,fut,m} - \bar{T}_{CM,ref,m}) \quad (4)$$

$$P_{adj,fut,d} = P_{obs,d} + (\bar{P}_{CM,fut,m} - \bar{P}_{CM,ref,m}) \quad (5)$$

Finally, daily data for future climate projections by GCMs under different greenhouse gas emissions scenarios for every station were used as inputs to the modified SWAT to project the watershed-scale changes in hydrological components in the 2040–2069.

## III. RESULTS AND DISCUSSION

### 3.1 Model calibration and verification

The SWAT model was calibrated based on daily measured discharge at 20 stations within the watershed. First, Sensitivity analysis Using SUFI-2 in SWAT-CUP was performed to evaluate the effect of parameters on the



performance of SWAT in the simulating runoff. So sensitivity analysis, Calibration, and validation of SWAT model were done for every station separately. Figure 2 compares graphically measured and simulated monthly surface runoff with 95% prediction uncertainty band for the calibration and validation period at 8 stations located in main outlets.

In addition to the visual comparison, the statistics of the results for the eight discharge stations above are given in Table 1. The overall  $N_{SE}$  and  $R^2$  for the calibration and validation periods indicated a close relationship between simulated monthly surface runoff with measured values. In general, based on the criteria presented by Moriasi et al., (2007), SWAT performed quite well in simulating surface runoff for the main stations.

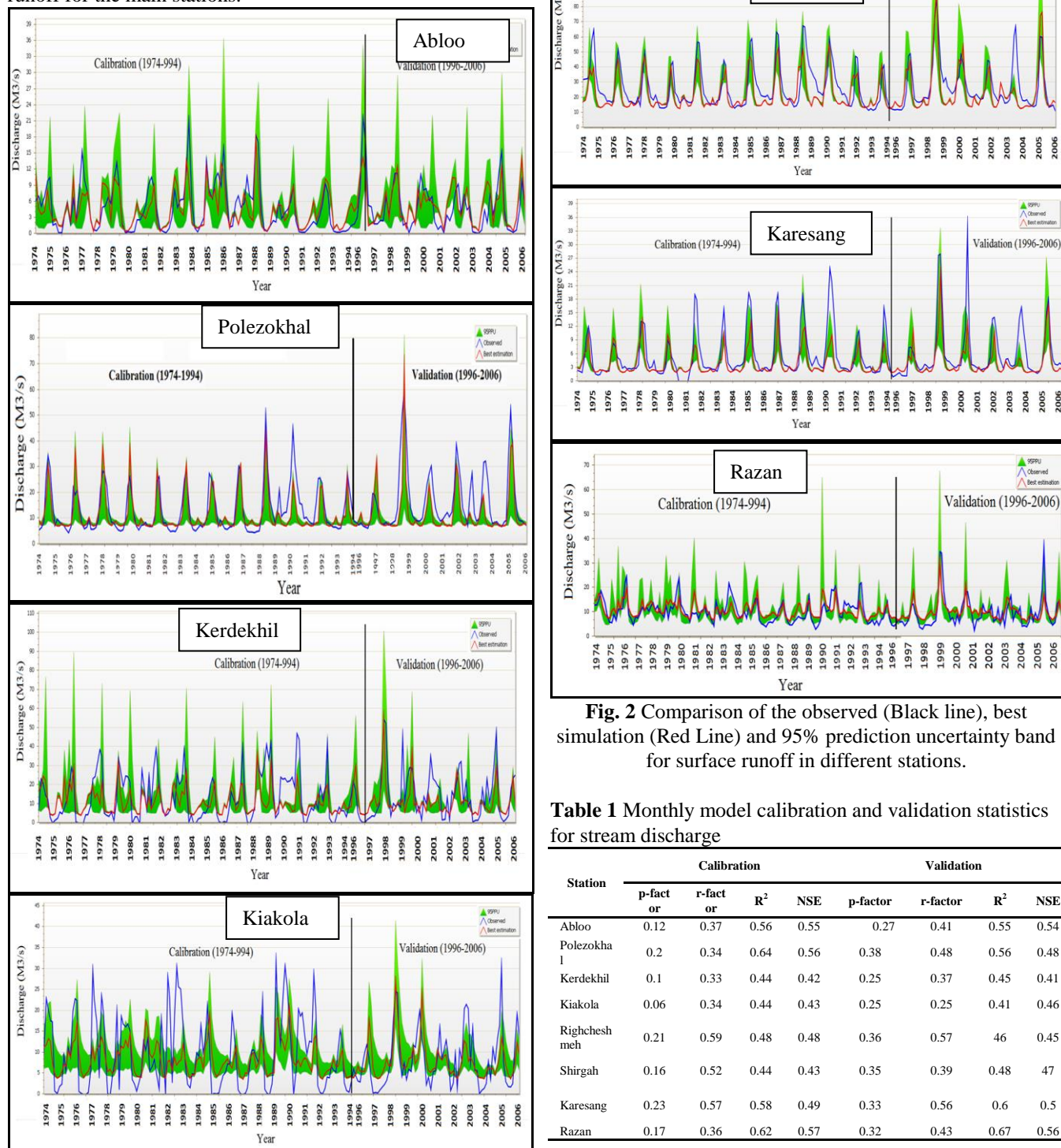


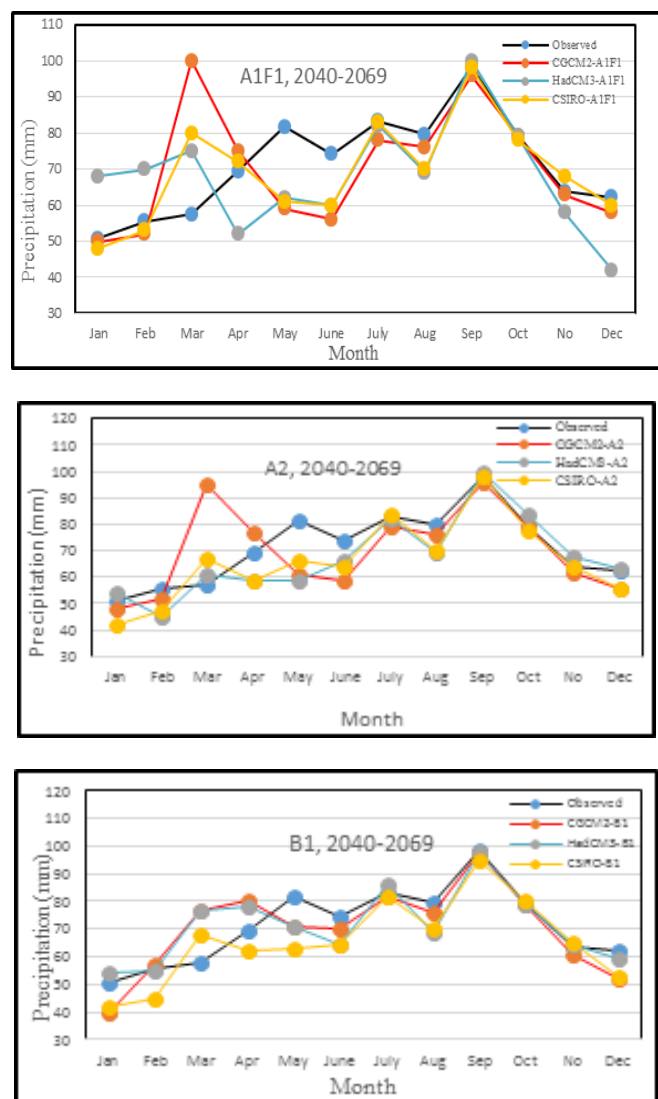
**Fig. 2** Comparison of the observed (Black line), best simulation (Red Line) and 95% prediction uncertainty band for surface runoff in different stations.

**Table 1** Monthly model calibration and validation statistics for stream discharge

Station	Calibration				Validation			
	p-factor	r-factor	R <sup>2</sup>	NSE	p-factor	r-factor	R <sup>2</sup>	NSE
Abloo	0.12	0.37	0.56	0.55	0.27	0.41	0.55	0.54
Polezokhal	0.2	0.34	0.64	0.56	0.38	0.48	0.56	0.48
Kerdekhil	0.1	0.33	0.44	0.42	0.25	0.37	0.45	0.41
Kiakola	0.06	0.34	0.44	0.43	0.25	0.25	0.41	0.46
Righcheshmeh	0.21	0.59	0.48	0.48	0.36	0.57	0.46	0.45
Shirgah	0.16	0.52	0.44	0.43	0.35	0.39	0.48	0.47
Karesang	0.23	0.57	0.58	0.49	0.33	0.56	0.6	0.5
Razan	0.17	0.36	0.62	0.57	0.32	0.43	0.67	0.56

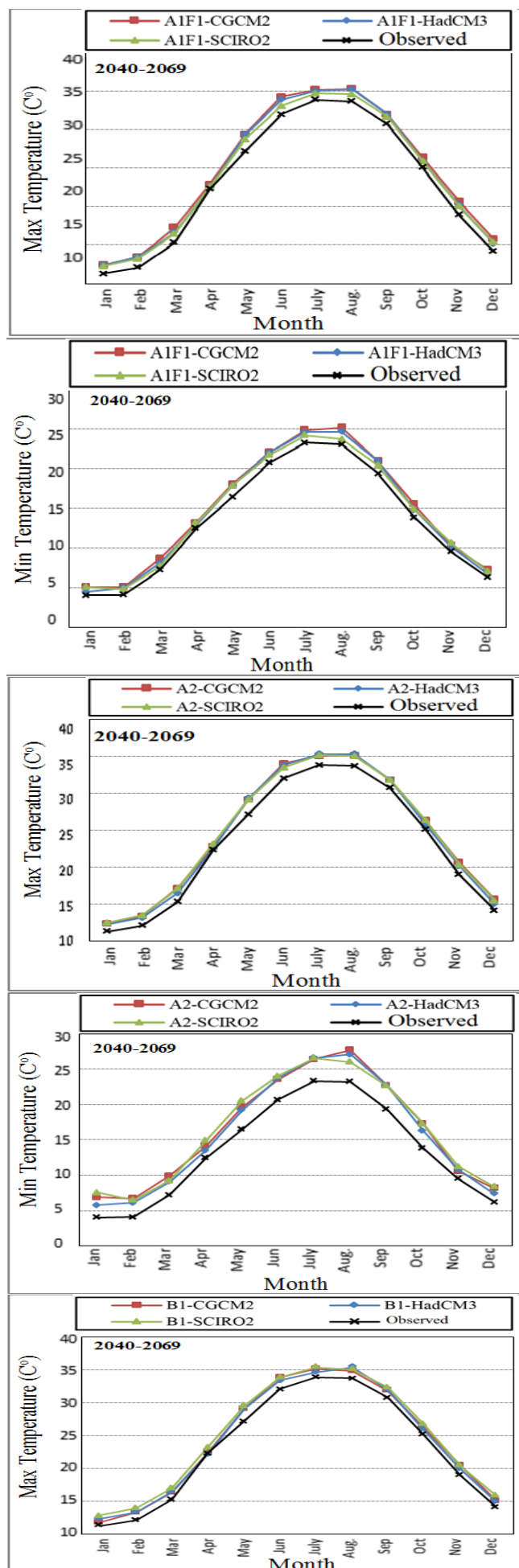
### 3.3 Impact of Climate Change on Temperature and Precipitation

Mean annual rainfall for all climate stations during the baseline 40-year period (1970-2010) was 731 mm. The minimum and maximum Mean annual rainfall in Mazandaran province were 578 and 1,307 mm in the east and west province, respectively. The average minimum and maximum daily temperature were 7/8 and 27.1 °C, respectively. In Figure 3 the predicted long-term average precipitations are compared with the historical data for different scenarios. As shown, major changes occur at the end of winter and spring, in Mars to June.



**Fig. 3** Comparison of average observed monthly precipitation for three GCMs for A2, B1 and A1F1 scenario

Figure 4 show average monthly changes in maximum and minimum temperature for three GCMs and for A1F1, A2 and B1 scenarios, respectively.  $T_{max}$  Increases in temperature for A1F1, A2 and B1 scenarios are 2.2, 2.1 and 2.1 °C and for  $T_{min}$  are 2.1, 3.5 and 2.1 °C, respectively. Monthly variation in temperature in figure 4 show that maximum increase for  $T_{max}$  predicted in June and August and minimum increase predicted in June and September. Whereas maximum increase for  $T_{min}$  predicted in August and minimum change predicted in November. In general, all projections show an increase in temperature over the basin.



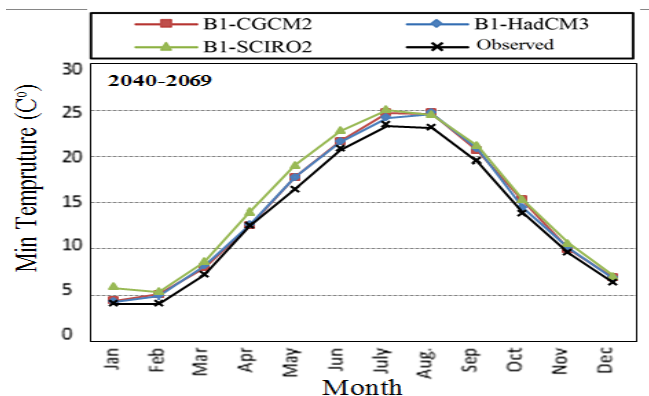


**Fig. 4** Comparison of maximum temperatures (left) and minimum temperatures (right) for three GCMs and for A1F1, A2, and B1 scenarios

### 3.4 Impact of Climate Change on Surface Runoff

Simulation results project a decrease in the annual surface runoff of 14.2% in the A2 scenario of CSIRO to an increase of 21.8% in B1 scenarios of HadCM3 for 2040–2069. But in

general, climate change impacts show an increase in surface runoff that has a different temporal pattern depending on the particular scenario and model (Table 2). The average change in annual surface runoff in the main outlets is -1.3%, 5% and -1.2% for A1F1, B1, and A2 scenario, respectively. The study conducted by Abbaspour et al. (2009) also reported that climate change may increase more frequent and larger-intensity floods in the wet regions of northern Iran. The monthly variation shows the increase in discharge is more pronounced in March and April and the decrease is more pronounced at the mid of spring to late summer (July-September) (Table 2). In other words, although study results show an increase in annual surface runoff, but it doesn't occur in a dry season. The increase of surface runoff in wet season and decrease in dry season was also concluded by Rahman et al. (2012), Yu and Wang (2009), Phan et al. (2011) and Shrestha et al. (2013) in different regions. Chang and Jung (2010) and Wu et al (2012) also reported that runoff and Water yield would increase in spring and substantially decrease in summer, respectively.

**Table 2** Predicted relative changes (percent of baseline levels) in monthly surface runoff by different GCMs

Model - Scenario	Jan	Feb	Mar	Apr	May	Jun	Jul	Aug	Sep	Oct	Nov	Dec	Ave.
CGCM2-A1F1	-2.4	-1	47.4	55.6	20.1	17.7	-3.5	-13.9	-12.8	-9	-1	-4.8	7.7
HadCM3-A1F1	-9.9	16.2	6.6	-2.9	-25.5	-33.5	-32.5	-28.8	-9.2	1.1	-12.1	-34.3	-13.7
CSIRO2-A1F1	3.1	-4.7	10.3	24.7	1.8	1.6	-7	-14.4	-17.6	-4.4	20.1	18	2.6
CGCM2-B1	-15	-3.5	20.9	37.1	21.1	23.2	8.8	0.5	1.4	10.8	0.2	-14.7	7.5
HadCM3-B1	8.1	7	24	38.2	21.7	25.9	31	11.3	-3.1	5.2	16	11.1	16.3
CSIRO2-B1	-1.5	-6	3	2.5	-20	-20.7	-30.2	-26.6	-28.6	-9.6	20.4	10.8	-8.8
CGCM2-A2	-3.2	-1.6	38.2	51.1	18	16.5	-2.6	-14.5	-11.8	-6.4	-0.3	-8.7	6.2
HadCM3-A2	21.4	3.4	12.7	4.6	-19.5	-24.8	-27.3	-23.2	-11.2	23.4	60.7	42.1	5.2
CSIRO2-A2	-10.3	-11.5	-3.8	-4.6	-25	-27.6	-32	-25.7	-23.8	-10.5	-2.5	-3.4	-15

Figure 5 presents the surface runoff Probability for baseline and GHGs scenarios for 10 surface runoff classes. Study results indicated that climate change may increase high values for discharge. As shown in figure 5, the probability of occurrence of high values in 10th class (more than 27.4 m<sup>3</sup>/s) from 0.3% for baseline has reached to 3%, 2.3% and 2.7% for A1F1, A2 and B1 scenarios for a period of 2040-2069. Whereas, the probability of occurrence for the most minimum surface runoff will decrease in this period. These results clearly indicated that climate change will treat water security by more floods and severe scarcity and droughts. The increase of high values of surface runoff also reported by (Perazzoli et al. 2012) in Brazil.

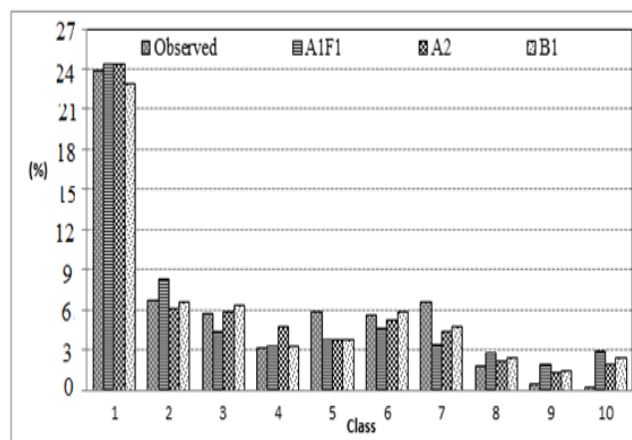


**Fig. 5** Surface runoff probability for baseline and GHGs scenarios in different GCMs.



#### IV. CONCLUSION

This study assesses the impact of climate change on surface runoff in the Mazandaran province basins in the north of Iran. To study the effects of climatic variations, the Soil and Water Assessment Tool (SWAT) model was implemented to simulate the present and future changes in surface runoff. The SUFI-2 algorithm in the SWAT-CUP program was used for parameter optimization. The climate change scenarios were constructed using outcomes of three General Circulation Models (CGCM2, HadCM3, and SCIRO2) for three emission scenarios (A1F1, A2 and B1). Calibration, validation and uncertainty analyses for discharge suggest that the SWAT model can be applied to simulate future changes in discharge due to climate change. Results indicated that differences between the climate models projections in surface runoff are high. The study results for 2040-2069 Compared with the present climate show an increase and decrease in an annual surface runoff with -1.3%, 5% and -1.2% for A1F1, A2, and B1 scenarios, respectively. Monthly variation shows that the increase in discharge is more pronounced in the wet season and the decrease at summer (July-September). The results of this study may be helpful to decision makers and other stakeholders for adaptive water resource management in a changing climate

#### REFERENCES

- [1] Abbaspour KC (2007) User manual for SWAT-CUP, SWAT calibration, and uncertainty analysis programs. Eawag: Swiss Fed. Inst. Of Aquat. Sci. and Technol. Du'bendorf, Switzerland.
- [2] Abbaspour KC, Faramarzi M, Ghasemi SS, Yang H (2009) Assessing the impact of climate change on water resources in Iran. *Water Resources Research* 45(10): W10434.
- [3] Arnold JG, Srinivasan R, Mutiah RS, Williams JR (1998) Large area hydrologic modeling and assessment part I: model development1. *Journal of the American Water Resources Association* 34(1): 73-89.
- [4] Azari M, Moradi H R, Saghaian B, Faramarzi M (2015) Climate change impacts on streamflow and sediment yield in the North of Iran. *Hydrological Sciences Journal*. DOI=10.1080/02626667.2014.967695.
- [5] Chang H, Jung IW (2010) Spatial and temporal changes in runoff caused by climate change in a complex large river basin in Oregon. *Journal of Hydrology* 388(3-4): 186-207.
- [6] Chen J, Brissette FP, Leconte R (2011) Uncertainty of downscaling method in quantifying the impact of climate change on hydrology. *Journal of Hydrology* 401(3-4): 190-202.
- [7] Dhar S, Mazumdar A (2009) Hydrological modeling of the Kangsabati river under changed climate scenario: a case study in India. *Hydrological Processes* 23(16): 2394-2406.
- [8] Fadaiey Khojaste M, Toghraie N, Pourmajidian M, Yazdi M (2010) Occurrence of Rhaeto-Liassic Gymnosperms flora (forests) of Shemshak formation in Kalat area, Golestan province, Northeastern Iran. *Iran J for Poplar Res* 18(3):485-497 (In Persian)
- [9] Ficklin DL, Luo Y, Luedeling E, Zhang M (2009) Climate change sensitivity assessment of a highly agricultural watershed using SWAT. *Journal of Hydrology* 374(1-2): 16-29.
- [10] Gosain A, Rao S, Basuray D (2006) Climate change impact assessment on the hydrology of Indian river basins. *Current Science* 90(3): 346-353.
- [11] Hamlet AF, Lettenmaier DP (2007) Effects of 20th-century warming and climate variability on flood risk in the western U.S. *Water Resour. Res* 43(6): W06427.
- [12] IPCC (2007) The Physical Science Basis. The contribution of Working Group I to the Fourth Assessment Report of the Intergovernmental Panel on Climate Change [Solomon S, Qin D, Manning M, Chen Z, Marquis M, Averyt KB, Tignor M, Miller HL (eds.)]
- [13] Jha M, Arnold JG, Gassman PW, Giorgi F, Gu RR (2006) Climate change sensitivity assessment on upper Mississippi river basin streamflows using SWAT. *JAWRA Journal of the American Water Resources Association* 42(4): 997-1015.
- [14] Kaini P, Nicklow JW, Schoof JT (2010). The impact of Climate Change Projections and Best Management Practices on River Flows and Sediment Load, ASCE.
- [15] Liu D, Zuo H (2012) Statistical downscaling of daily climate variables for climate change impact assessment over New South Wales, Australia. *Climatic Change*: 1-38.
- [16] Mitchell TD, Carter TR, Jones PD, Hulme M, New M (2004) A comprehensive set of high-resolution grids of monthly climate for Europe and the globe: the observed record (1901-2000) and 16 scenarios (2001-2100). Tyndall Centre Working Paper.
- [17] Moriasi D, Arnold J, Van Liew M, Bingner R, Harmel R, Veith T (2007) Model evaluation guidelines for systematic quantification of accuracy in watershed simulations. *Transactions of the ASAE* 50 (3): 885-900.
- [18] Nash JE, Sutcliffe JV (1970) River flow forecasting through conceptual models part I. A discussion of principles. *Journal of Hydrology* 10(3): 282-290.
- [19] Perazzoli M, Pinheiro A, Kaufmann V (2012) Assessing the impact of climate change scenarios on water resources in southern Brazil. *Hydrological Sciences Journal*. 1-11.
- [20] Phan, D, Wu C, Hsieh S (2011) Impact of climate change on stream discharge and sediment yield in Northern Viet Nam. *Water Resources* 38(6): 827-836.
- [21] Rahman M, Bolisetti T, Balachandrar R (2012) Hydrologic modeling to assess the climate change impacts in a Southern Ontario watershed. *Canadian Journal of Civil Engineering* 39(1): 91-103.
- [22] Shrestha B, Babel MS, Maskey S, van Griensven A, Uhlenbrook S, Green A, Akkharath I (2013) Impact of climate change on sediment yield in the Mekong River basin: a case study of the Nam Ou basin, Lao PDR. *Hydrol. Earth Syst. Sci.* 17(1): 1-20.
- [23] Wu Y, Liu S, Abdul-Aziz O (2012) Hydrological effects of the increased CO2 and climate change in the Upper Mississippi River Basin using a modified SWAT. *Climatic Change* 110(3-4): 977-1003.
- [24] Yu PS, Wang YC (2009) Impact of climate change on hydrological processes over a basin scale in northern Taiwan. *Hydrological Processes* 23(25): 3556-3568.
- [25] Zarghami M, Abdi A, Babaeian I, Hassanzadeh Y, Kanani R (2011) Impacts of climate change on runoffs in East Azerbaijan, Iran. *Global and Planetary Change* 78(3-4): 137-146.